Sidelobe Modulation Scrambling Transmitter Using Fourier Rotman Lens

Zhang, Y., Ding, Y., & Fusco, V. (2013). Sidelobe Modulation Scrambling Transmitter Using Fourier Rotman Lens. IEEE Transactions on Antennas and Propagation, 61(7), 3900-3904. [6484901]. DOI: 10.1109/TAP.2013.2254453

Published in:
IEEE Transactions on Antennas and Propagation

Document Version:
Early version, also known as pre-print

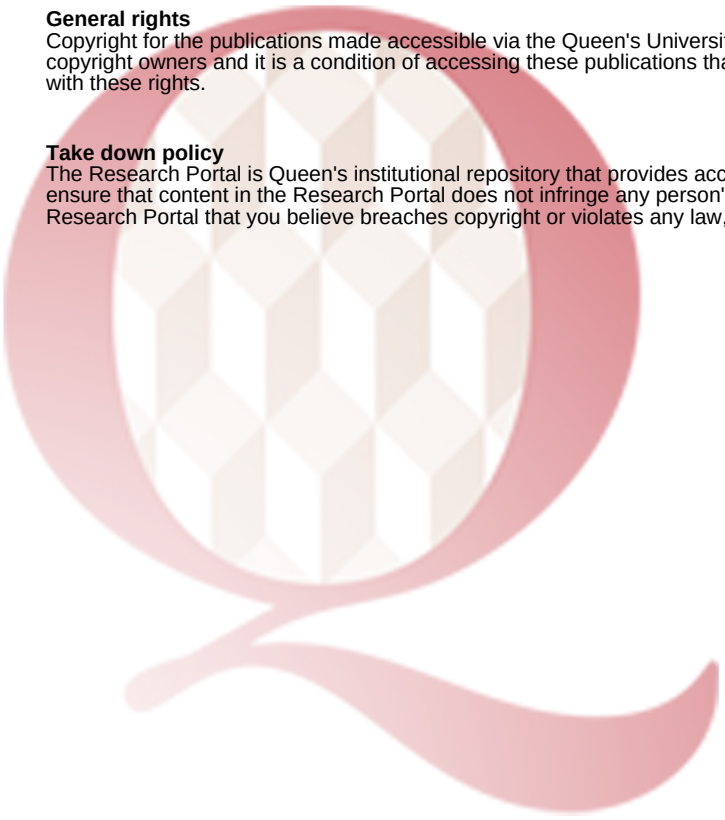

Sidelobe Modulation Scrambling Transmitter using Fourier Rotman Lens

Yunhua Zhang, Yuan Ding, and Vincent Fusco, *Fellow, IEEE*

***Abstract*—A means for scrambling the digital modulation content in the sidelobes of a radio transmission from a steerable antenna array is presented. The method uses a Fourier transform beam-forming network simultaneously excited by an RF information stream and orthogonally injected interference streams. The proposed system is implemented using a Fourier Rotman lens and its operational characteristics are validated for a 10 GHz QPSK transmission.**

***Index Terms*— Fourier transform beamforming, physical layer security, Rotman lens.**

I. Introduction

The demand for high level secure wireless communication systems is an imperative [1]. In addition to encryption imposed at application layers the adoption of physical layer security techniques can add more challenges to eavesdropper attempts to intercept and successfully decipher useful information. Recently several physical-layer spatial encryption technologies have been proposed [2]-[8]. Here physical layer data security is realized by distorting the IQ plane constellation diagram of the transmitted signal in all spatial directions except along a pre-specified direction in order to hamper data decoding in all directions except the pre-specified one.

In [2] and [3], spatial data encryption is achieved for phase and amplitude modulated signals respectively by transversely placing active phase conjugating lens (or lenses) between transmitters and receivers. However, the frequency bandwidth of modulated signals is limited by the inherent narrow bandwidth of analog phase conjugating lenses. Furthermore, the secure communication direction cannot be scanned except by mechanically rotating the system. Other physical-layer spatial encryption technologies, under the banner of directional modulation (DM), have been suggested in [4]-[8]. To date DM systems have been implemented by using passive parasitic arrays [4], [5] or actively driven arrays of phased antennas [6]-[8]. In both methods the transmission phase characteristics of each element in the radiating array is updated on a symbol-by-symbol basis. Consequently symbol encoding is extremely demanding from an RF design perspective, since the use of multiple RF switches and digital phase shifters poses a major complexity challenge.

A Fourier transform based beam-forming network (FT-BFN), such as a Butler matrix [9], [10] has the capability to simultaneously produce multiple beams which are orthogonal in the beam space. In the context of this paper the benefit of beam orthogonality is that it allows a mechanism whereby far field sidelobe modulation content can be scrambled while leaving steered main beam information content unaffected. The recently introduced Fourier constrained Rotman lens [11], [12] provides a means for achieving this functionality in a way that is readily scalable by both frequency of operation and array port aperture size using simple 2-D printed circuit board technology. This is not readily possible with high order Butler matrix designs, [9], where multilayer board technology is required. Consequently we will use the Fourier constrained Rotman lens as the vehicle for discussion in this paper. Hence the Fourier Rotman network architecture is briefly introduced in Section II, while in Section III, the properties of the proposed sidelobe scrambling transmitter is discussed with respect to the QPSK modulation scheme. This is followed in Section IV by experimental validation of the system. Further discussions are provided in Section V. Finally, summaries and conclusions are drawn.

II. Sidelobe Scrambling Architecture Based on Fourier Transform Network

The concept of spatial distortion of IQ constellations of transmitted digital symbols in all directions other than in a pre-assigned transmission direction is shown in Fig.1.

Instead of inserting phase conjugating lenses [2], [3] or imposing baseband information data directly within the RF front-end stage, e.g., through the use of switches embedded within passive or actively driven antenna structures [4], [5], [7], [8], or, RF phase shifters [6], [13], [14], an alternative, much simpler, transmitter architecture, depicted in Fig. 2, based on a FT-BFN is now proposed. It is noticed that only two RF chains are needed in this architecture. One is for information data

Manuscript received November 9, 2012. This work was sponsored by the Queen's University of Belfast High Frequency Research Scholarship and the UK Engineering and Physical Research Council grant EP/H049606/1.

Yunhua Zhang, was with the Institute of Electronics, Communications and Information Technology (ECIT), Queen's University of Belfast, Belfast, United Kingdom, BT3 9DT. He is now with the School of Electronic Information, Wuhan University, Wuhan, China, 430072 (e-mail: zhangyunhuawhu@hotmail.com)

Yuan Ding, and Vincent Fusco are with the Institute of Electronics, Communications and Information Technology (ECIT), Queen's University of Belfast, Belfast, United Kingdom, BT3 9DT (phone: +44(0)2890971806; fax: +44(0)2890971702; e-mail: v.fusco@qub.ac.uk; yding03@qub.ac.uk).

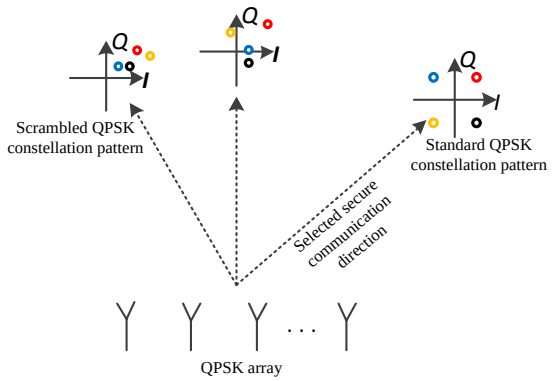

Fig 1. Illustration of deliberate spatial QPSK constellation distrotion. Along a user specified direction a usable constellation is formed. Away from the desired direction the constellation is scrambled.

insertion, and the other is utilized to inject orthogonal sidelobe scrambling interference into the system. As illustrated in Fig. 2, useful information is projected along the main beam generated by the FT-BFN, which points to the desired secure communication direction. This directionally projected information is unaffected, due to FT-BFN beam orthogonality properties, by the interference signals injected at all other FT-BFN ports. On the other hand, the sidelobes of the useful information beam, i.e. those which lie along the undesired directions, are severely distorted both in amplitude and phase by the interference signals. The result of this is to give distorted constellation diagrams along all directions other than along the prescribed main beam direction. With the Fourier Rotman lens, as the FT-BFN, beam steering to a new communication direction can be achieved by selecting a new injection (beam) port and redistributing the interference signals to the remaining unused (beam) ports. The steering angular resolution is determined by the number of ports in the FT-BFN.

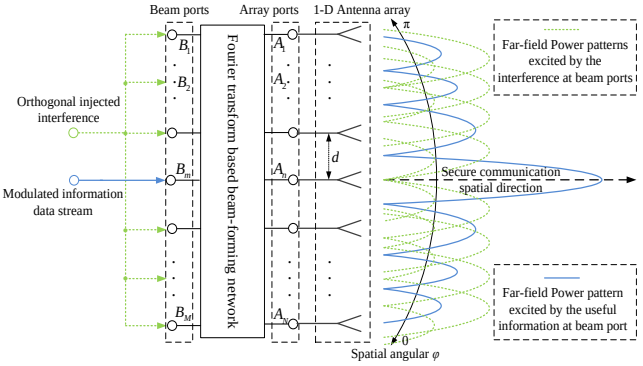

Fig 2. Proposed Fourier transform beam forming network (FT-BFN) sidelobe scrambling architecture.

The Fourier Rotman lens has recently been shown to have significantly superior orthogonality properties when compared to a classical Rotman lens, [11]. In a Fourier transform network, the signal at the n^{th} array port (A_n) is contributed to by all the excitations at the beam ports through relationship [11], re-stated here as,

$$A_n = \sum_{m=1}^{M} B_m \cdot e^{-j\frac{2\pi}{N}\left(n-\frac{N+1}{2}\right)\left(m-\frac{M+1}{2}\right)} \quad (1)$$

where B_m is the injected signal, e.g., the information signal or the interference signal in Fig. 2, at the m^{th} beam port. M and N are the number of the beam ports and the array ports respectively. In this paper M=N. The phase reference of the output in the Fourier transform network is chosen to be the array port geometric center.

With the array excitations known through (1), the array factor $AF(\varphi)$ of a 1-D antenna array with uniform spacing d can be expressed as

$$AF(\varphi) = \sum_{n=1}^{N}\left\{\left[\sum_{m=1}^{M} B_m \cdot e^{-j\frac{2\pi}{N}\left(n-\frac{N+1}{2}\right)\left(m-\frac{M+1}{2}\right)}\right]\cdot e^{j\frac{2\pi}{\lambda_0}\left(n-\frac{N+1}{2}\right)\cdot d\cdot\cos(\varphi)}\right\} \quad (2)$$

In (2), λ_0 is the free space wavelength at the working frequency of the system.

III. Simulation under QPSK Modulation

Next the properties of the proposed system will be studied for QPSK modulation. First a theoretical model of a Fourier Rotman lens equipped with 13 beam ports and 13 array ports set to work at 10 GHz with antenna element spacing of $\lambda_0/2$=15mm is established. Arbitrarily we select the 5th beam port for excitation with a QPSK signal stream at 0 dBm power level. The choice of the 5th beam port for excitation leads to a pattern maximum at 72º. Simultaneously all of the other beam ports are excited by identical interference signals consisting of identical constant amplitude −10 dB (relative to the QPSK carrier) sine wave at 10 GHz. The −10 dB level was chosen to be approximately the same level as first set of array sidelobes. The phase of the injected interference signal is updated using randomly selected (from a uniform distribution) phases within the range from 0º to 360º on a per symbol basis. The magnitudes and the phases of AFs for each QPSK symbol are calculated by (2), and are depicted in Fig. 3. For comparison with the experiment results in the next section, the random interference phases in this simulation example are set to be 25º, 70º, 125º and 40º for each QPSK symbol. As shown in Fig. 3(a), the AF magnitudes for the four different symbols overlap each other only at 13 discrete spatial angles, which correspond to the main beam directions excited by each of 13 beam port in the Fourier lens. The magnitudes at the crossover points are determined by the magnitudes of the injected information or interference signals, namely 0 dB or −10 dB in this example. At other spatial angles they markedly differ from each other. Moreover, as shown in Fig. 3(b), the phase differences between different symbols are also distorted by the randomly phased interference injection except in a small range around 72º where they are held close to 90º. At the 12 orthogonal directions (magnitude crossover directions) other than the information direction (72º) the phases are inevitably equal to the phases of the injected interference for each symbol, which in a real system is updated randomly at the modulation rate. These results suggest that

QPSK constellation patterns should be optimally available only along the 72º direction, while along all other directions they should no longer form a standard central-symmetric square in the IQ plane.

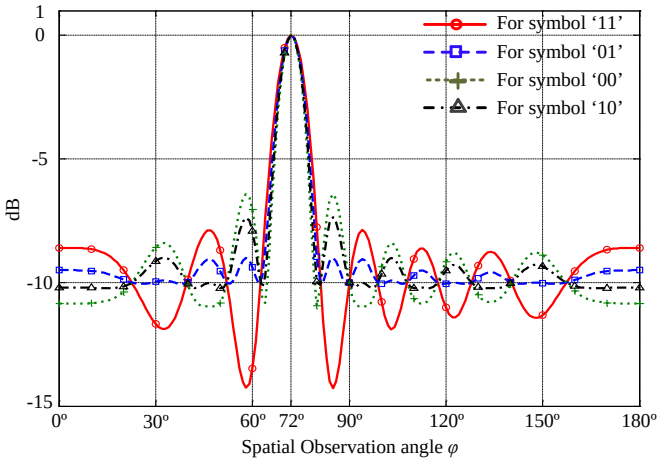

(a) *AF* magnitude patterns for each QPSK symbol

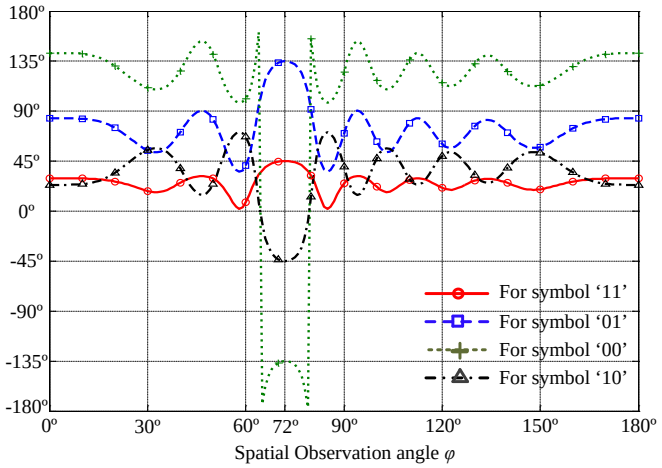

(b) *AF* phase patterns for each QPSK symbol

Fig 3. The *AF* magnitude and phase patterns for each of the four different QPSK symbols sent by a DM transmitter configured for 72º beam projection with −10dB random phased interference injection at all other beam ports.

IV. Experimental Validation

To validate the theoretical simulation results in Section III, a 13 by 13 Fourier transform constrained Rotman lens for 10 GHz operation whose design and fabrication details are given in [11] was used, Fig. 4. Using its measured S-parameters, the normalized *AF*s for each beam port excited separately were computed and are presented in Fig. 5. The beam orthogonality properties of the lens can be observed, e.g. along the direction of the 5th beam, here 72º, total interference beam leakage from all other beam ports is below −20 dB. Fig. 6 shows the *AF* magnitudes and phases for each of the different QPSK symbols with the same interference settings as for the simulation in the last section. Here near-equal amplitude *AF* responses occur at 72º while phase differences are held between 89º and 93º only along this direction.

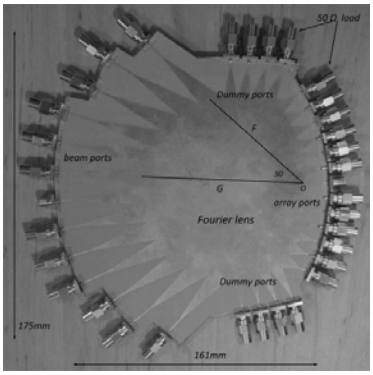

Fig 4. The fabricated Fourier transform constrained Rotman lens for operating at 10 GHz.

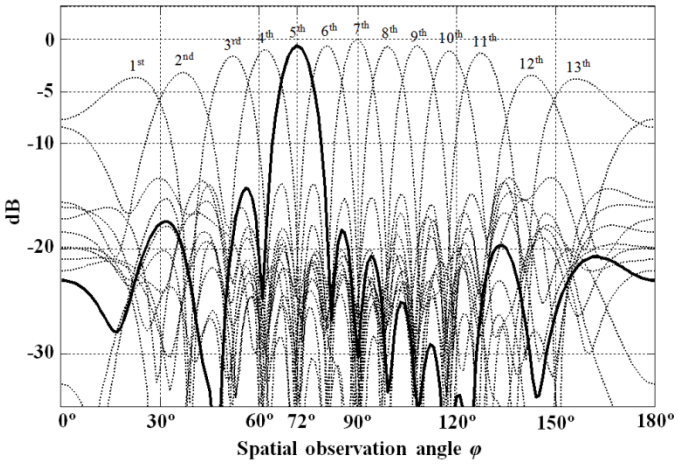

Fig 5. *AF*s for each beam port excited separately based on measured lens S-parameters ('—': the *AF* with the excitation at the 5th beam port; '- - -': the *AF*s with the excitations at the other beam ports).

V. Discussions

Next the transmitter's capability for scrambling the constellation diagrams at the directions other than the desired communication direction needs to be quantified. To do this we use a figure of merit, denoted as $FOM(\varphi)_{DM}$, for describing the distortion of the received constellation diagram:

$$FOM_{DM} = \left[\frac{\frac{1}{T}\sum_{j=1}^{T} \left| S_{DM\_j} - S_{id\_j} \right|^2}{\frac{1}{T}\sum_{j=1}^{T} \left| S_{id\_j} \right|^2} \right]^{\frac{1}{2}} \quad (3)$$

Here S_{DM_j} is the actual received symbol when the j^{th} symbol is transmitted, whereas the S_{id_j} is the corresponding j^{th} ideal received symbol. T is the total number of transmitted symbols, set to be 5000 for the graphs below. At each specified spatial direction, the total power received from the transmitter is normalized to be identical to that received from an ideal QPSK system, namely

$$\sum_{j=1}^{T} \left| S_{DM\_j} \right|^2 = \sum_{j=1}^{T} \left| S_{id\_j} \right|^2 \quad (4)$$

Furthermore, as would happen during the standard QPSK synchronization process, each received constellation pattern is rotated to align the phase of the reference symbol. Hence

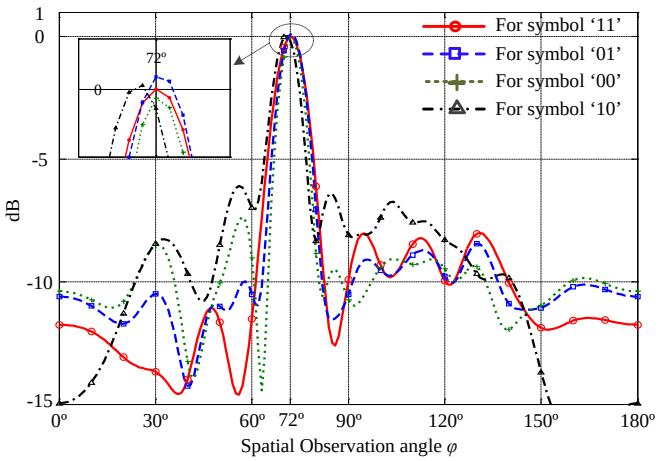

(a) *AF* magnitude patterns for each QPSK symbol

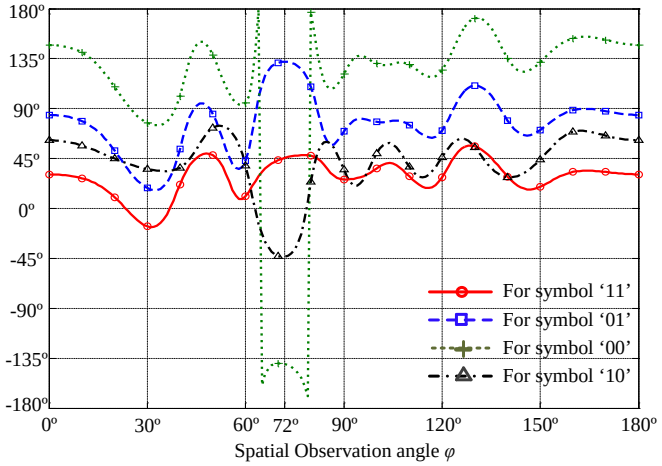

(b) *AF* phase patterns for each QPSK symbol

Fig 6. The magnitudes and phase patterns of *AF*s based on measured S-parameters of the Fourier Rotman lens for 4 different QPSK symbols with −10 dB interference injection at each remaining beam ports.

$FOM(\varphi)_{DM}$ describes the average normalized distance from the received symbols relative to those of the ideal constellation points along each prescribed direction φ. With the above definition an $FOM(\varphi)_{DM}$ value of 0 means that all received symbols lie exactly on top of the ideal QPSK constellation patterns while higher values indicate that the received symbols are more grossly distorted in amplitude and/or phase relative to ideal QPSK constellation symbol position. Thus $FOM(\varphi)_{DM}$ is used to quantify symbol displacement in IQ space due to spatially dependent scrambling. It should be noted that in a conventional system *EVM* is used to quantify symbol displacement along a fixed direction accounting for effects due to noise and system non-linearities. Due to the extra capability of the constellation pattern manipulation possessed by a DM transmitter, the FOM_{DM} does not link to the system *BER* via the relationship stated in [15] as *EVM* does.

Fig. 7 shows the $FOM(\varphi)_{DM}$ for the fabricated Fourier Rotman lens transmitter over observation angles 0º to 180º for different interference power levels for QPSK transmission with no noise introduced in the channel. It is noticed that as more interference energy is injected, the higher the $FOM(\varphi)_{DM}$ values are along non-preferred wireless communication directions. The non-zero $FOM(\varphi)_{DM}$ value at 72º is caused by the imperfections in magnitude and phase relationships introduced by lens fabrication errors which reduce beam orthogonality.

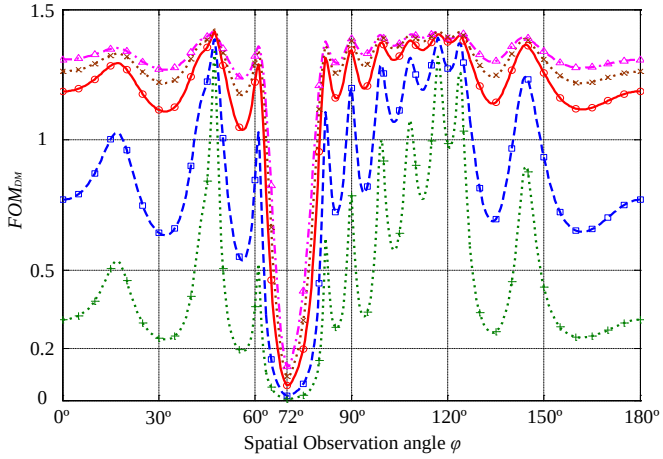

Fig 7. Fourier Rotman lens DM transmitter $FOM(\varphi)_{DM}$ curves as a function of interference power levels ('-△-': −3 dB; '-×-': −6 dB; '-○-': −10 dB; '--□--': −20 dB; '-+-': −30 dB).

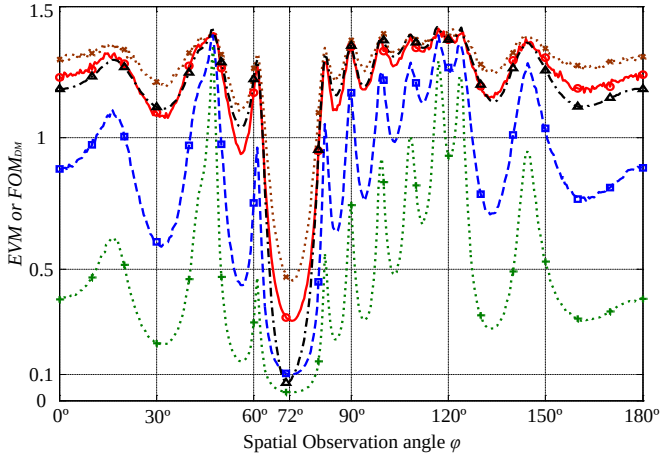

Fig 8. Fourier Rotman lens conventional transmitter $EVM(\varphi)$ curves as a function of *SNR* ('-+-': 30 dB; '--□--': 20 dB; '-○-': 10 dB; '-×-': 6 dB) and Fourier Rotman lens DM transmitter $FOM(\varphi)_{DM}$ curve ('--△--': 30 dB *SNR* and −10 dB interference at each 12 beam port).

When no interference is injected into the Fourier Rotman lens the system can be configured as a conventional transmitter. Consequently $FOM(\varphi)_{DM}$, becomes equivalent to standard $EVM(\varphi)$, and is constant and equal to zero when the channel is noise free. In free space with consideration of additive Gaussian noise, the $EVM(\varphi)$ under different signal to noise ratio (*SNR*), signal power is selected along the main beam direction, is obtained and depicted in Fig. 8. To maintain consistency, the percentage representation for *EVM* is not adopted here. It can be observed that the impact of the channel noise on the $EVM(\varphi)$, Fig. 8, is similar to that of the injected interference on the $FOM(\varphi)_{DM}$, Fig. 7, except along the pre-specified communication direction since the channel noise is in the case of the conventional transmitter arrangement uniformly distributed in the whole space. At the main beam direction, 72º

in this example, *EVM* is determined by *SNR* via $EVM = SNR^{-1/2}$ [15]. For comparison with the non-interference and 30 dB *SNR* case, under the Gaussian wireless channel of 30 dB *SNR*, the $FOM(\varphi)_{DM}$ of the DM system with −10 dB interference injection at each of the 12 beam port is also illustrated in Fig. 8. Without being affected at the selected secure direction, $FOM(\varphi)_{DM}$ has deteriorated at all other directions, indicating scrambling on received constellation patterns. Across most spatial regions $FOM(\varphi)_{DM}$ approximates to the $EVM(\varphi)$ of the non-interference case for *SNR*<10dB. Since the interference can be considered as a multiplicative noise in the system, the normal strategy of reducing distance between transmitter and receiver to improve *SNR*, and hence the *EVM*, does not lower FOM_{DM}. Therefore no assistance to eavesdroppers in the recovery of DM encoded information content is forthcoming.

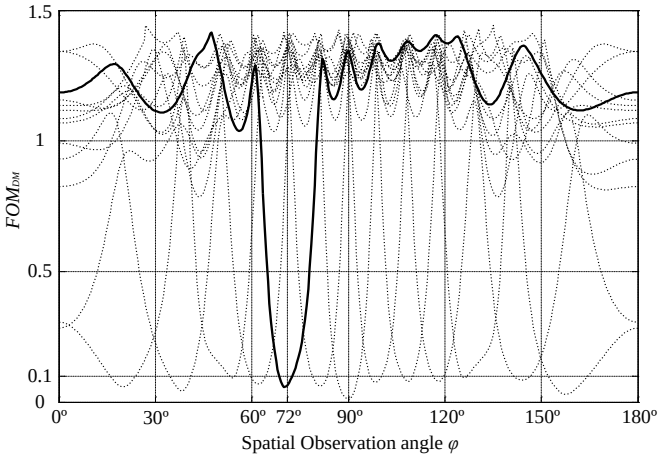

Fig 9. Fourier Rotman lens DM transmitter $FOM(\varphi)_{DM}$ curves for information injected sequentially at each beam port, with the remaining ports being injected with interference.

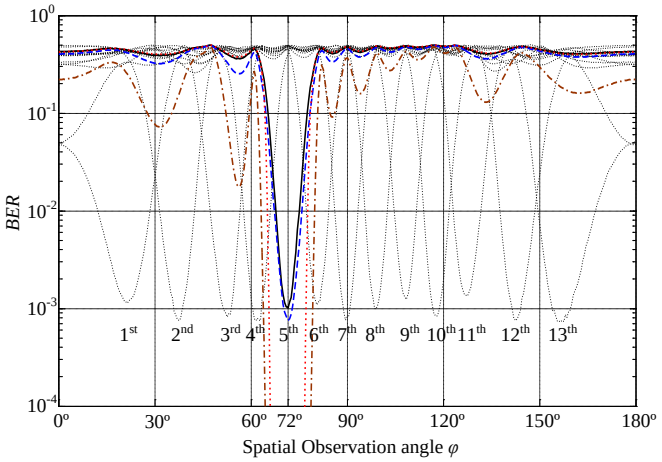

Fig 10. Fourier Rotman lens DM transmitter *BER* curves for information applied sequentially at each beam port, with each of the remaining ports injected with interference (‘ ····· ’: 10 dB *SNR* and −10 dB interference, information injected at each beam port other than the 5th; ‘ —— ’: 10 dB *SNR* and −10 dB interference, information injected at the 5th beam port; ‘ ····· ’: 20 dB *SNR* and −10 dB interference, information injected at the 5th beam port;). The Fourier Rotman lens conventional transmitter *BER* curves for information injected at the 5th beam port (‘ – – – ’: 10 dB *SNR* with no interference; ‘ –·–·– ’: 20 dB *SNR* with no interference) are also shown.

Fig. 9 shows the $FOM(\varphi)_{DM}$ curves when different beam ports are selected for steered useful information transmission in different spatial directions. The interference at each remaining beam port is set to be −10 dB, and the channel noise is not included.

To further assess system performance and also validate the figure of merit, $FOM(\varphi)_{DM}$, proposed in this paper we investigate, for a Gaussian wireless channel *SNR* 10 dB and 20 dB, the *BER* spatial distributions for information applied at each beam port. *BER* simulation are conducted using a data stream length of 10^6, Fig. 10. A standard QPSK demodulator is assumed, which decodes received symbols based on within which quadrant the constellation points lie. To permit direct comparison with Fig. 9, the interference at each remaining beam port is also set to be −10 dB. It is observed that $FOM(\varphi)_{DM}$ can well predict the *BER* performance of the DM system. Also illustrated in Fig. 10 with regards to the *BER* beamwidths and sidelobe levels, using 5th beam port excitation as an example, the *BER* performance of the DM Rotman system is superior to operation with no orthogonal interference injection.

VI. Conclusion

By employing a FT-BFN only two RF chains are required in order to obtain physical layer DM operation. The use of a Fourier Rotman lens significantly simplifies scrambling transmitter architecture design, while retaining the potential for beam steering. The use of a 2-D printed circuit board Fourier transform lens makes physical realization simple as well as readily scalable with regard to frequency and aperture size. The scheme presented in this paper should find application in enhanced communications systems where data security is of concern.

Acknowledgment

The authors thank Mr. Michael Major for the fabrication of the Fourier transform constrained Rotman lens. The authors also would like to thank the anonymous reviewers for their valuable comments and suggestions to improve the quality of the paper.

References

[1] A. Khisti and G. W. Wornell, “Secure Transmission With Multiple Antennas-Part II: The MIMOME Wiretap Channel,” *IEEE Trans. Inf. Theory*, Vol. 56 No. 11, Page(s): 5515-5532, Nov. 2010.

[2] O. Malyuskin and V. Fusco, “Spatial Data Encryption Using Phase Conjugating Lenses,” *Antennas and Propagation, IEEE Transactions on*, vol. 60, pp. 2913-2920, 2012.

[3] O. Malyuskin and V. Fusco, “Amplitude modulated signal transmission through a phase conjugating lens,” *Microwaves, Antennas & Propagation, IET*, vol. 6, pp. 1026-1033, 2012.

[4] A. Babakhani, D.B. Rutledge and A. Hajimiri, “Transmitter Architectures Based on Near-Field Direct Antenna Modulation,” *Solid-State Circuits, IEEE Journal of*, vol. 43, pp. 2674-2692, 2008.

[5] A. Babakhani, D. Rutledge and A. Hajimiri, “Near-field direct antenna modulation,” *Microwave Magazine, IEEE*, vol. 10, pp. 36-46, 2009.

[6] M.P. Daly and J.T. Bernhard, "Directional Modulation Technique for Phased Arrays," *Antennas and Propagation, IEEE Transactions on*, vol. 57, pp. 2633-2640, 2009.

[7] M.P. Daly and J.T. Bernhard, "Beamsteering in Pattern Reconfigurable Arrays Using Directional Modulation," *Antennas and Propagation, IEEE Transactions on*, vol. 58, pp. 2259-2265, 2010.

[8] M.P. Daly, E.L. Daly and J.T. Bernhard, "Demonstration of Directional Modulation Using a Phased Array," *Antennas and Propagation, IEEE Transactions on*, vol. 58, pp. 1545-1550, 2010.

[9] J. Butler and R. Lowe, "Beam forming matrix simplifies design of electronically scanned antennas," *Electronic Design*, vol. 9, pp. 170-173, April 1961.

[10] Chia-Chan Chang, Ruey-Hsuan Lee and Ting-Yen Shih, "Design of a Beam Switching/Steering Butler Matrix for Phased Array System," *Antennas and Propagation, IEEE Transactions on*, vol. 58, pp. 367-374, 2010.

[11] Y. Zhang and V. Fusco, "Fourier transform using Rotman lens," *Proceeding of the 42nd European Microwave Conference*, pp. 715-718. Amsterdam, Netherland, Oct.28th - Nov. 2nd 2012.

[12] Y. Zhang, S. Christie, V. Fusco, R. Cahill, G. Goussetis and D. Linton, "Reconfigurable beam forming using phase-aligned Rotman lens," *Microwaves, Antennas & Propagation, IET*, vol. 6, pp. 326-330, 2012.

[13] HongZhe Shi and T. Alan, "Direction dependent antenna modulation using a two element array," in *Antennas and Propagation (EUCAP), Proceedings of the 5th European Conference on*, pp. 812-815, 2011.

[14] HongZhe Shi and T. Alan, "An Experimental Two Element Array Configured for Directional Antenna Modulation," in *Antennas and Propagation (EUCAP), Proceedings of the 6th European Conference on*, pp. 1624-1626, 2012.

[15] R.A. Shafik, S. Rahman and AHM Razibul Islam, "On the Extended Relationships Among EVM, BER and SNR as Performance Metrics," in *Electrical and Computer Engineering (ICECE), International Conference on*, pp. 408-411, 2006.